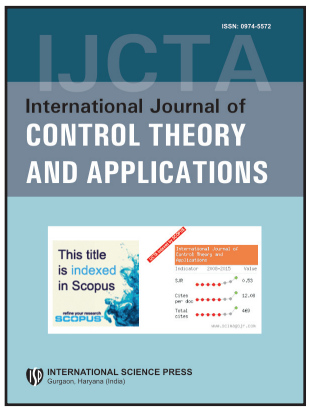

International Journal of Control Theory and Applications

ISSN : 0974-5572

Volume 10 • Number 24 • 2017

Dynamic Simulation of an Optimally Sized Standalone Wind/PV/Fuel Cell/Battery System

D. Suchitra[a], R. Jegatheesan[b], Soumyadeep Nag[c] and Nidhi A Kumar[d]

[a]*Assistant Professor, Department of Electrical and Electronics Engineering, SRM University, Chennai-603203, India. Email: such1978@yahoo.com*
[b]*Professor, Department of Electrical and Electronics Engineering, SRM University, Chennai-603203, India. Email: jegainche@gmail.com*
[c]*PG Scholar, Department of Electrical and Electronics Engineering, SRM University, Chennai-603203, India. Email: soumyadeepnag@gmail.com*
[d]*PG Scholar, Department of Electrical and Electronics Engineering, SRM University, Chennai-603203, India. Email: minikukku@gmail.com*

Abstract: Energy management strategy of a standalone hybrid system plays a crucial role in controlling the power flow from various power storage equipment and supervises the power dispatch process so that the degradation of life of power storage elements can be prevented or slow down. In this paper a wind/PV/fuel cell/battery system has been optimally sized using Particle Swarm Optimization (PSO) and a new energy management strategy for the optimally sized hybrid back-up system has been proposed. The design variables for optimal sizing are number of wind turbines, number of PV modules, number of fuel cells, number of batteries, volume of hydrogen and Depth of Discharge (DOD) of batteries. The energy management strategy divides the operation of the system into four different modes: Hybrid mode, Fuel cell mode, Battery mode and Renewable recharge mode. The change between different modes is governed by a central power flow controller which checks the set points of load, State of charge (SOC) of battery current and volume of hydrogen and then generates reference power signals for the storage elements. In this paper a new method for characteristic adjustment of solar modules using PSO has been adopted and a neural network implemented MPPT strategy using a dc-dc boost converter for solar panels has been implemented and compared with the classical Perturb and observe (P&O) method which displays appreciable improvement in the performance of the solar panels. With the help of dynamic modeling of fuel cells, electrolyzer, batteries, solar modules and wind turbines, a dynamic simulation of the system has been carried out using MATLAB/SIMULINK environment in order to observe the operation of the energy management strategy. The results describe the operation of an optimally sized combination of wind/PV/fuel cell/battery system under the different modes of operation.

Keywords: Energy management strategy, MPPT, Electrolyzer, Boost converter, Hybrid Energy system.

1. INTRODUCTION

Adoption of hybrid renewable energy systems is essential for the growth of economy. The main sources of renewable energy are Solar and Wind Energy. These two sources are complimentary in nature, also, the pattern or

duration of solar power coincides with the load pattern. However, these sources are intermittent and unpredictable; besides, the efficiency of these energy conversion systems are not very impressive. Thus, to take full advantage of these sources, power storage devices are to be used. Power storage devices consist of battery, fuel cell, super capacitors etc. either used individually or as a combination to form a hybrid backup source.

The techno-economic problem of optimal sizing has been solved by many researchers in different ways using different tools. A hybrid simulated annealing – Tabu search method for optimal sizing for autonomous power system was presented where a hybrid optimization tool received great attention along with various constraints like initial cost, unmet load, and operational constraints like battery set point for diesel generator charging etc [1, 2, 3, 4, 5]. An optimal sizing has been performed for a wind/PV/battery system using an improved PSO which introduces the concept for restart and disturbance in PSO. The use of Loss of Power Supply Probability (LPSP) to measure systems reliability has been attempted[6]. Similar problem has also been solved using genetic algorithm [7]. The authors have proposed a unique standalone hybrid wind solar power generation system, characterized by Phase Locked Loop (PLL) control and dump power control [8]. Among the various parameters used to judge a combination of hybrid system, the LPSP, LCE and ACS were very often referred in the literature [11, 12, 13]. An hourly basis analysis has been performed, instead of a monthly average method [1] or a worst month method [10], which helps to avoid over sizing.

Recently the use of hybrid power storage has become a key area of research. In this work, the main purpose of using a hybrid storage system is to elongate the life of the major storage elements. Another reason for supporting the fuel cell with the battery bank is to enhance its dynamic response [14]. Thus, in this paper a hybrid back-up is formed with fuel cell stack and battery, where the fuel cell is considered as the major back-up source. Hydrogen fuel and Proton Exchange Membrane (PEM) Fuel cells have their own advantages over other forms of energy storage. In comparison to commonly used battery storage, Hydrogen is well suited for seasonal changes, because of its inherent high mass energy density and longevity of energy storage. Unlike batteries where charging can only be done with extra power generated by renewable energy, hydrogen can be added externally to the hydrogen tank by the operator. The high energy density of hydrogen fuel makes PEM fuel cells highly advantageous. Further, the addition of an electrolyzer helps to increase the reliability of the system. Fuel cells are eco-friendly as water is the only by product.

This paper focuses on obtaining optimal sizing of wind/PV/fuel cell/battery system, followed by the dynamic simulation of the system. The design variables considered are: number of wind turbines, number of PV panels, number of fuel cells, number of batteries, depth of discharge of batteries and the volume of hydrogen stored. Two parameters such as the Expected Energy not served (EENS) and per unit cost are used to represent the reliability and the cost of energy respectively. These two parameters help to judge a particular combination in a techno-economical manner and hence to solve the problem of optimal sizing. Data sheets from the manufacturers have been considered as the input data and characteristic curves have been used for data extraction and parameter calculation as presented in [15-17]. The energy flow controller ensures the operation of the system under various modes considering various constraints[29][32][33].

This paper also reports a neural network based MPPT algorithm for Photovoltaic modules. A feed forward neural network has been trained with Levenberg Marquardt algorithm [18] to produce the current reference for the panels and simultaneously produce maximum power by using a DC-DC boost converter. The ANN implemented method is reported to be extremely fast and more efficient as compared to the classical P&O method.

The power flow controller forms the heart of any energy system. The design of the implemented power flow controller is as shown in Figure 1. To verify the validity of optimally sized system during real time, the dynamic analysis has been performed using simulation in MATLAB/SIMULINK environment. Through the

dynamic simulation, this paper has attempted to verify the operation of the energy management strategy and the obedience of the device set points.

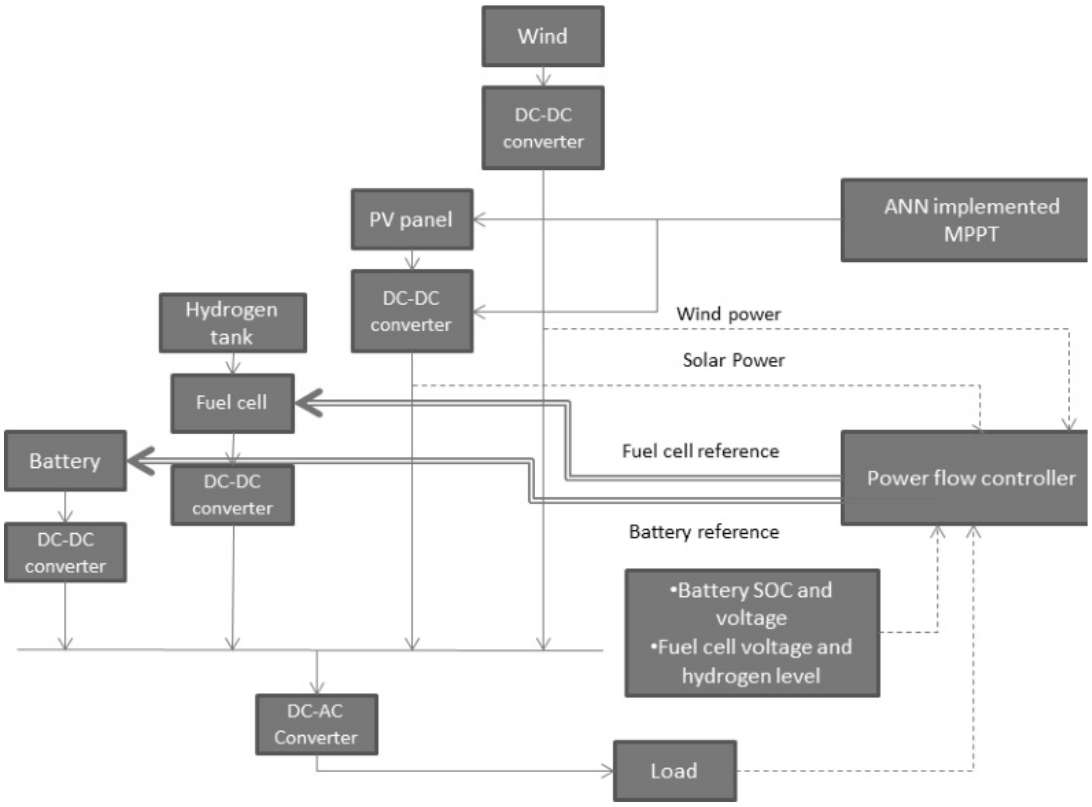

Figure 1: Schematic Diagram of the hybrid system

2. STEADY STATE MODELING OF EQUIPMENT

2.1. Modeling of Solar Modules

Like other semiconductor devices, solar cells are also affected by temperature. Any increase in temperature causes a reduction in band gap, hence an increase in dark current [21]. The importance of Loss Factor (LF) has been realized in [19, 20], where different kinds of dust such as ash, red soil, etc. have been deposited over the solar panels. As a result of dust accumulation, open circuit voltage reduces by 5% to 25% [20]. The equation for solar power is given by:

$$P_{PV} = P_N \,.\, G_t \,.\left(1 - \left(\frac{C_t}{100(TC - TN)}\right)\right).\, NS \,.\, \frac{NP}{LF} \,.\, effinv \tag{1}$$

where, P_N is the nominal power, G_t is the hourly radiation, C_t is the temperature coefficient of the panel, TC is the cell temperature, NS and NP are the number of the modules in series and parallel. LF is in the range of 1.1 to 2. Although inverter efficiency (*effinv*) of the inverter varies with load, its value is assumed to be 0.98, TN is the temperature for maximum power output, NS has been fixed as 2, while NP has been considered as a design variable for optimization. The cell temperature is calculated by using:

$$TC = T_{amb} + \frac{G_t\,(NCOT - 20)}{800} \tag{2}$$

where, T_{amb} is the ambient temperature, and NCOT is the normal cell operating temperature which is fixed as 47°C.

2.2. Modeling of Wind turbines

The amount of mechanical power captured by a wind turbine is given by [26]:

$$P_{WT} = 0.5 C_P(\lambda, \beta)\rho(T) A V^3 \tag{3}$$

where, V is the incoming wind velocity, A is the area swept by blades of the turbine which is considered as $27m^2$. ρ, the air density, has been assumed to remain constant at 1.39 kg/m^3. The conversion efficiency or power coefficient of a turbine C_p is a function of the tip-speed ratio λ and pitch angle β. Mathematically, tip-speed ratio λ is the ratio of the tip speed of the turbine blades to wind speed is given by:

$$\lambda = \frac{\omega_m R}{v} \tag{4}$$

where, ω_m is the turbine rotational speed in mechanical radians/second and R is the radius of the turbine in meters. While extracting the maximum power from the turbine, the value of the pitch angle β is kept constant (around 0), to ensure maximum possible turbine output.

2.3. Modeling of Fuel Cells

To model the steady state characteristics of the PEMFC, a detailed model [22], using the data in the user manual, has been simulated. The results of this simulation, i.e., the power output of the fuel cell, have been plotted against the consumption of hydrogen and the efficiency of the device. Piecewise Curve fitting has been performed on the graph of power output vs. Hydrogen consumption and the coefficients A_{FC} and B_{FC} have been derived for (5) and (6). The steady-state fuel cell system modeling has been performed with the help of A_{FC}, B_{FC} constants as follows:

$$\text{cons}_{fc} = A_{FC} \,.\, P_{N_{FC}} + B_{FC} \,.\, P$$

$$\text{If} \quad P_{output} < P_{max\_eff} \tag{5}$$

$$\text{cons}_{fc} = B_{FC} \,.\, P_{N_{FC}} + A_{FC} \,.\, P\left(1 + F_{ef}\left(\frac{P}{P_{N_{FC}}} - \frac{P_{max\_eff}}{100}\right)\right)$$

$$\text{If} \quad P_{output} > P_{max\_eff} \tag{6}$$

where, A_{FC} and B_{FC} are the Power coefficients of values 0.05 kg/kW and 0.004 kg/kW respectively for the fuel cell, P_{max_eff} is the rated power output of the fuel cell at maximum efficiency, P_{output} is the output power of the fuel cell, F_{ef} is the Faraday's efficiency, P is the power to be supplied by the fuel cell, P_{NFC} is the nominal rating of the fuel cell and $cons_{fc}$ is the consumption of hydrogen.

2.4. Modeling of Batteries

The steady state model of a battery depends on the state of charge (SOC) of the battery [27][28].The change in SOC of the battery is given by:

$$SOC(t + \Delta t) = SOC(t) \,.\, (1 - \delta) + I_{bat}(t)\Delta t \eta_{bat} \tag{7}$$

where, δ is the self discharge coefficient, η_{bat} is the efficiency of the battery which is taken as 0.93 and $I_{bat}(t)$ is the battery current in the previous step.

The maximum current the battery can provide at a particular time instant is given by:

$$I_{batmax}(t+\Delta t) = \max\left[0, \min\left\{I_{max}, \left(\frac{c}{\Delta t} SOC_{max} - SOC(t)\right) + (SOC - SOC_{min})\frac{1-c}{\Delta t}\right\}\right] \quad (8)$$

where, I_{max} is the maximum charging current,

$$c = \begin{cases} 1 \text{ battery is charging} \\ 0 \text{ battery is discharging} \end{cases}$$

and

$$SOC_{max} = N_{batp} C_N \quad (9)$$

$$SOC_{max} = N_{batp} C_N (1 - DOD) \quad (10)$$

where, N_{batp} is the number of batteries in parallel, C_N is the nominal capacity and DOD is the depth of discharge of the battery.

2.5. Modeling of Electrolyzers

The rate of gas production is based on the Faraday's law of electro-chemical reaction.

Cathode reaction:

$$2H_2O(l) + 2e^- \rightarrow H_2(g) + 2OH^-(aq.) \quad (11)$$

Anode reaction:

$$2OH^-(aq.) = \frac{1}{2} O_2(g) + H_2O(l) + 2e^- \quad (12)$$

Faraday's efficiency is often known as current efficiency. In this paper the Faraday's efficiency has been assumed to be between 92% and 98% [26]. For the steady state modeling of the 2 kW electrolyzer, the amount of hydrogen produced is given by:

$$H_{2\,prod_{elec}} = A_{elec} \cdot P_{N\_elec} + B_{elec} \cdot P \quad (13)$$

where, A_{elec} and B_{elec} are the Power coefficients of values 0.025 kg/kW and 0.1 kg/kW respectively for the electrolyzer, $P_{N\,elec}$ is the nominal power of the electrolyzer and P is the power input to the electrolyzer.

3. PSO IMPLEMENTED OPTIMAL SIZING

3.1. Calculation of Judgment Parameters

Considering the techno – economic nature of the problem, reliability and per unit cost are considered as the parameters for optimal sizing. The Expected value of Energy Not Served (EENS) represents the reliability of the system and ranges from 0 to 1 indicating complete reliability and complete unreliability respectively. Per unit cost gives us the cost of one unit of energy.

EENS for a combination is given as:

$$EENS_{nc} = \frac{\sum_1^{8760} ENS}{Totalload} \quad (14)$$

where, ENS = Load(t) – Total Generation(t) (15)

Per unit cost has been calculated as follows:

$$\text{Perunit cost(\$/kWh)} = \frac{\sum_{k=1}^{4}(\text{I}_k + \text{O \& M}_k - \text{S}_k)\ \text{Rated Capacity} \times \text{D}_k}{\text{N} \times (\text{Total load})} \tag{16}$$

where, *nc* is the number of combinations, ENS is the Energy not supplied, I_k is the initial cost of the k^{th} component, $\text{O\&M}_k$ is the Operation and maintenance cost for the k^{th} component, $\text{S}_{\underline{k}}$ is the Salvage cost of the k^{th} component, N is the total number of years and D_k is the replacement frequency

3.2. Formulation of a Single Objective Function

A combination is chosen as the best combination by equally compromising both objectives, namely, EENS and Per unit cost (pucost). Since the ideal value of EENS and Per unit cost should be minimized, the problem can be reduced to a single objective optimization problem and stated as:

$$\text{Min } f = \sqrt{f_1^2 + f_2^2} \tag{17}$$

where, f_1 is the Expected value of Energy Not Served and f_2 is the Per unit cost.

3.3. Coding Strategy of PSO

PSO is one the most powerful and versatile tools of optimization in terms of speed of optimization, ideology of the optimization process and the computational burden. It was first brought about by Kennedy and Eberhart [23] and is based upon the flocking or feeding behavior of birds. The use of evolutionary algorithms eases the procedure of solving the problem with the derivatives and also reduces the time required to solve a problem by reducing the computational burden.

PSO consists of the following main steps:

Step 1: The particles have been initially randomly placed in the entire search space which included all four dimensions [d_1, d_2, d_3, d_4. The particles indicated by $\lambda = 1, 2, 3, 4, \ldots$, were given positions in each dimension as [$x_{\lambda, d1}$, $x_{\lambda, d2}$, $x_{\lambda, d3}$, $x_{\lambda, d4}$]. The global best and the population size is initialized.

Step 2: Position update of the particles have been done using:

$$x_{\lambda, d}^{i} = x_{\lambda, d}^{i-1} + v_{\lambda, d}^{i-1} \tag{18}$$

Step 3: Function evaluation with each particle is performed by

$$f = obj(\text{EENS, pucost}) \tag{19}$$

Step 4: Global best (gbest) and Particle best (pbest) have been updated after evaluating the function.

Step 5: Velocity is updated using

$$\text{V}_{\lambda, d}^{i} = \left(w\text{V}_{\lambda, d}^{i-1}\right) + \left(c_1\left(\text{pbest} - x_{\lambda, d}^{i}\right)\right) + \left(c_2\left(\text{gbest} - x_{\lambda, d}^{i}\right)\right) \tag{20}$$

where, c_1 and c_2 are personal and global cognitive factors and w is inertia.

Step 6: Inertia is updated using

$$w = w_{\max} - (i(w_{\max} - w_{\min})/\text{N}) \tag{21}$$

where, N is the maximum number of iterations, and i is the value of current iteration. The steps from 2 to 6 is repeated till the objective is reached.

4. DYNAMIC MODELING OF EQUIPMENT

4.1. Modeling of Solar Modules

The dynamic model of solar cells consists of the light generated current, dark reverse saturation current and leakage current. The current of a solar cell, as a function of voltage is given as [9][15]:

$$I_{pv} = I_{Ph} - I_O\left[\exp\left(\frac{V_d}{V_t}\right) - 1\right] - \frac{V_d}{R_P} \tag{22}$$

where, I_{Ph} is the photo current, I_O is the diode reverse saturation current, V_t is the thermal voltage, R_p is the parallel resistances, I_{pv} is the output current and V_d is the diode voltage of the cell.

The light generated photo current I_{Ph} is given by:

$$I_{Ph} = I_{sc}\left[1 + K_i\left(T - T_n\right)\right] \times \left(\frac{G}{G_n}\right) \tag{23}$$

where, I_{sc} is the cell's short circuit current, K_i is the temperature coefficient of cell's short circuit current, T is the cell's absolute temperature, T_n is the reference temperature, G and G_n are the solar radiation at actual and nominal level respectively.

The diode reverse saturation current is given by:

$$I_0 = \frac{I_{sc}}{\exp\left(\frac{V_{oc}}{V_t}\right) - 1}\left(\frac{T}{T_n}\right)^3 \exp\left[\left(\frac{E_g}{V_t}\right)\left(\frac{1}{T_n} - \frac{1}{T}\right)\right] \tag{24}$$

where, V_{oc} is the cell's open circuit voltage, E_g is the band gap energy of the semi conductor used in the cell and V_t is the thermal voltage, given by:

$$V_t = \frac{\alpha k T}{q} \tag{25}$$

where, q is the electric charge (1.6×10^{-19} C), α is the cell idealising factor (1.1) and k is the Boltzmann's constant (1.38×10^{-23} J/K).

4.2. Modeling of Fuel Cells and Electrolyzers

The Proton Exchange Membrane based Fuel Cell (PEMFC) model used in this study is based on the dynamic PEMFC stack model, which was developed and validated in [22][30].The following equation models the fuel cell voltage (V_{fc}):

$$V_{fc} = E_{oc} - N \times A \times \ln\left(\frac{i_{fc}}{i_0}\right) \cdot \frac{1}{sT_d/3 + 1} \tag{26}$$

where, E_{oc} is the open circuit voltage, N is the number of cells, A is the Tafel Slope, i_0 is the exchange current, T_d is the response time (at 95% of the final value in seconds) and i_{fc} is the fuel cell current.

The hydrogen produced by each cell during electrolysis process is given by:

$$H_2 = (i \times t \times 22.4 \times \eta_F)/(96485.30 \times 2) \text{ in litre} \tag{27}$$

where, i is the current supplied to the electrolyzer, t is the time duration, η_F is the Faraday's effieciency.

4.3. Modeling of Batteries

The battery is modelled using a controlled voltage source in series with a constant resistance as in [16][31].The open voltage source is calculated with a non-linear equation based on the actual SOC of the Lead-Acid battery. The battery voltage obtained is given by :

$$E = E_o - K\left[\frac{Q}{Q - \int i\,dt}\right] + A \times \exp\left(-B\int i\,dt\right) \tag{28}$$

$$V_{bat} = E - R \times i \tag{29}$$

where, V_{bat} is the battery voltage, E_0 is the battery constant voltage, K is the polarisation constant, Q is the maximum battery capacity, $\int i\,dt$ is the actual battery charge, R is the internal resistance, i is the battery current, A is the exponential zone amplitude and B is the exponential zone time constant inverse.

The three necessary points used to extract the model parameters are[16]:

- the fully charged voltage (E_{full})
- the end of the exponential zone (E_{exp} and Q_{exp})
- the end of the nominal zone (E_{nom} and Q_{nom})

The unknown parameters are calculated as:

$$A = E_{full} - E_{exp} \tag{30}$$

$$B = 3/Q_{exp} \tag{31}$$

$$K = \frac{E_{full} - E_{nom} + A\left(\exp\left(-BQ_{nom}\right) - 1\right).\left(Q - Q_{nom}\right)}{Q_{nom}} \tag{32}$$

$$E_o = E_{full} + K + Ri - A \tag{33}$$

5. ENERGY MANAGEMENT STRATEGY

The division of energy between the fuel cell and the battery is done such that initially the battery is made to supply the load completely (thereby increasing the life of the fuel cell). If in case the discharge current exceeds the maximum discharge current (260 A for one battery), the remaining power in excess of renewable energy will be shared equally between the fuel cell and battery. The fuel cell remains on until the discharge current reduces to 13 A for one battery. Figure 2 displays the energy management strategy.

The energy management strategy displays the operation of the system in four different modes, namely:

- **Battery mode:** Batteries are given priority for discharge as they are comparatively less costly. This mode is followed when the load is in excess of power generated by the renewable energy sources and battery SOC is between SOC_{min} and SOC_{max}. Here the battery discharges gradually as SOC reaches SOC_{min}. Now it is checked whether the discharge current is in excess of maximum discharge current of the battery or not. The battery is discharged only if the discharge current is below the maximum discharge current. In this case, the battery alone satisfies the load in excess of renewable sources.
- **Fuel cell mode:** This mode is followed when the load is in excess of power generated by the renewable energy sources and the battery SOC is less than or equal to SOC_{min}. The other requirements of the mode are that the volume of hydrogen must be within limits and that the power required for the fuel cell should be below or equal to its rated power.

- **Hybrid mode:** The hybrid mode is designed such that the fuel cell starts working as soon as the battery discharge current exceeds the maximum discharge current. Here both, the battery as well as the fuel cell are working and the load in excess of renewable energy is halved. This mode ensures that battery life is prolonged as SOC_{min} is reached more slowly as compared to the case where this mode is absent, thus reducing the number of cycles. This mode is followed until the discharge current reduces to 13 A for one battery.

$$P_{fc} = P_{bat} = 0.5 \times \text{Total demand} \tag{34}$$

- **Renewable Recharge mode:** In this mode the renewable energy is in excess of the load and this excess energy is used to charge the batteries. In case the batteries are fully charged the excess energy is then used to run the electrolyzer to generate hydrogen.

Key features of this strategy are:

- **Battery:** A cycle of a battery consists of one complete discharge and recharge. By implementing the concept of load sharing, the SOC_{min} is reached more slowly and enhancing the life of the battery is enhanced by limiting the number of cycles. The terminal voltage of the battery is automatically taken care of by this mode.
- **Fuel cell:** With the help of load sharing, fuel cell life is extended. Moreover, the fuel cell power output lies around its maximum efficiency point during most of its operational hours.

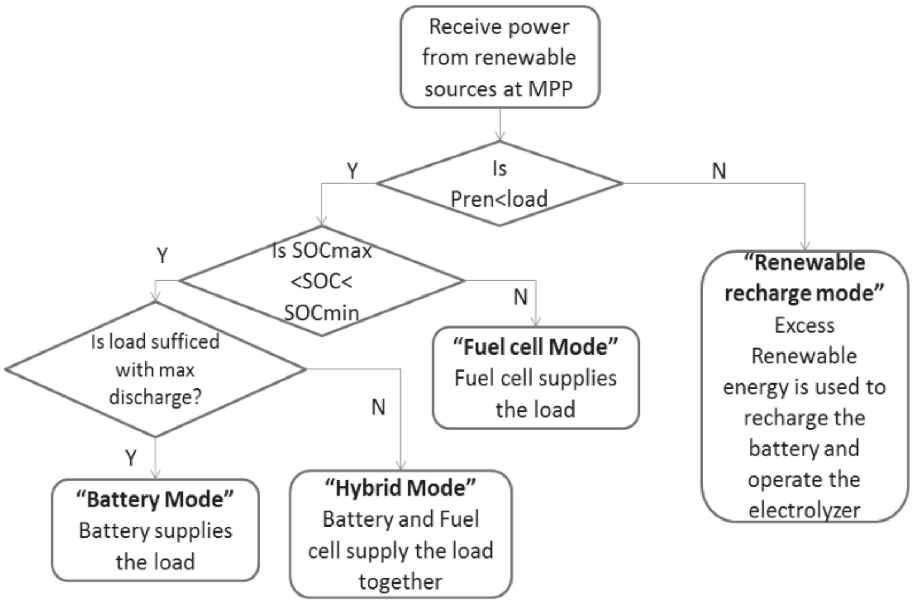

Figure 2: Energy management strategy

6. ANN IMPLEMENTED MPPT FOR SOLAR MODULES

In the literature, there are two methods for implementing the P&O algorithm: the direct method (duty ratio perturbation) and the indirect method (reference voltage/current perturbation). In the direct method, the MPP is searched by continuously perturbing the duty cycle of the dc–dc converter. Although the main advantage of the direct method is its simplicity, it has a slower transient response and a worst performance at rapidly changing irradiance compared with the indirect method [24]. The choice of step size in P&O decides the performance of the algorithm. Due to a large step size, although, the MPP is reached fast, the oscillations at the end of MPP will

reduce the accuracy and increases the time elapsed for the system. Further, the search for MPP might proceed into the wrong direction and hence reduce the power output of the system. When a small step size is chosen, the number of iterations increases due to which the time take taken to reach the MPP increases.

The MPPT for PV panels, as depicted in Figure 3, is performed by a feed forward neural network trained with Levenberg – Marquardt training algorithm. The Levenberg–Marquardt algorithm blends the steepest descent method and the Gauss–Newton algorithm. Fortunately, it inherits the speed advantage of the Gauss–Newton algorithm and the stability of the steepest descent method [25]. More than 10000 samples of tabulated data consisting of: radiation, temperature, as inputs, and I_{ref} as the output was built, where radiation was varied in steps of 5 W/m^2 and the temperature was varied in steps of 1K, in order to construct the training data sheet of the neural network and an MSE of .001 was achieved.

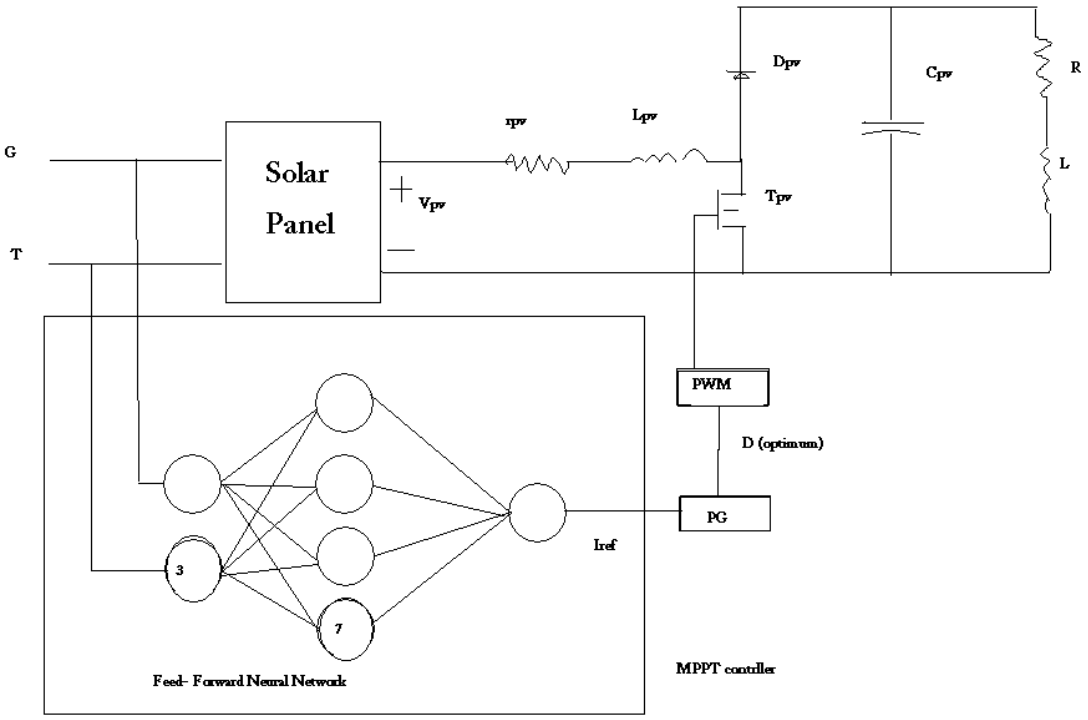

Figure 3: Algorithm for ANN implemented MPPT

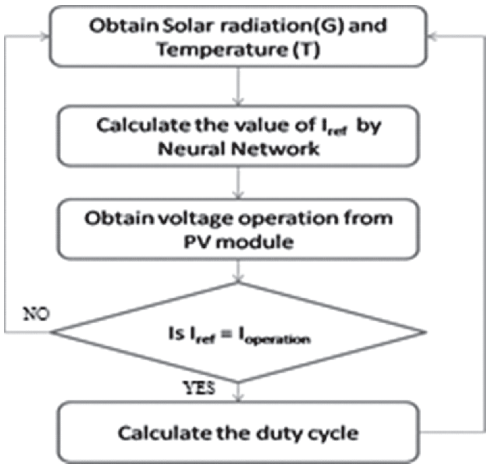

Figure 4: Algorithm for ANN implemented MPPT

7. RESULTS

7.1. Results of Optimal Sizing

The Wind speed, Temperature and Solar radiation data for 8760 Hours of Kolkata (22.5667°N, 88.3667°E), India, taken from the meteorological department are shown in Figures. 5-7. Kolkata experiences high temperature during summer and comparatively low temperatures during the months of winter. The average wind speed lies around 5 m/s with a peak wind speed of 25 m/s. The sample load data considered for optimization is shown in Figure 8.

The component specifications such as rating, cost and the limits of the number of components used are given in Table 1. The various PSO parameters involved in the optimization of reliability and cost are given in Table 2.

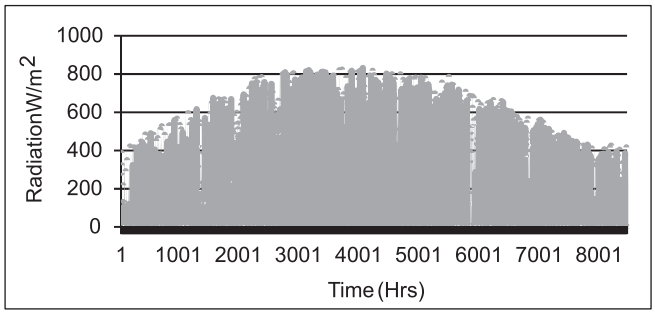

Figure 5: Solar radiation for 8760 hrs

Table 1
Component specifications, cost and limits on number of components

Equipment	*Capacity*	*Initial cost*	*Replacement cost*	*O&M cost*	*Lifetime*	*Minimum*	*Maximum*
Wind turbine	5 kW	1015 $/kW	230 $/kW	25 $/kW	15	1	3
PV modules	200 W	4401 $/kW	880 $/kW	88.01 $/kW	20	2	100
Fuel cell stack	6 kW	6000 $/kW	300 $/kW	240 $/kW	15000	1	3
Battery	250 Ah	200 $	20 $	5 $	–	4	40
Electrolyzer	2 kW	3000 $/kW	150 $/kW	150 $/kW	10	1	1
Hydrogen storage	–	990 $/kg	–	10 $/yr	50	.24	4
DOD	–	–	–	–	–	.6	.2

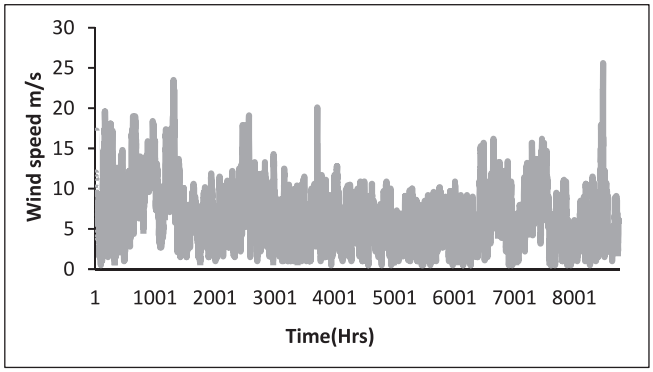

Figure 6: Wind speed data for 8760 hrs

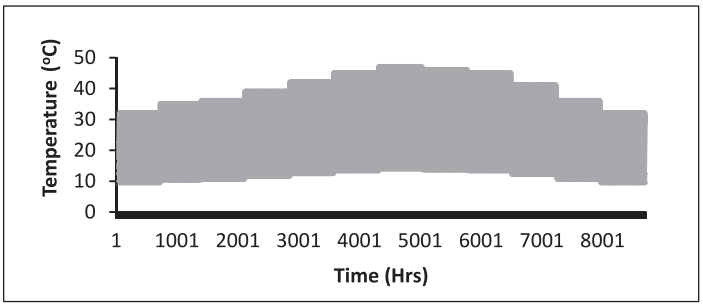

Figure 7: Temperature data for 8760 hrs

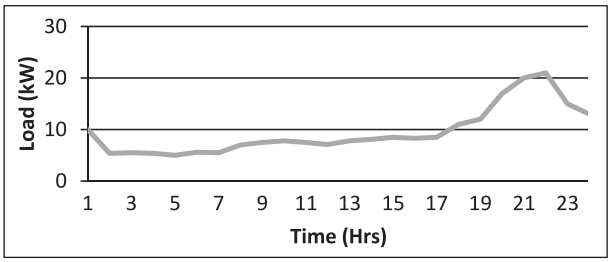

Figure 8: Load data for 24 hours, standard IEEE domestic load profile

Table 2
Parameters of PSO

Parameter	*Value*
Local cognitive factor c1	2
Global cognitive factor c2	2
Population size	49
Iterations	50
Inertia weight min & max	0.1 & 1

The optimal sizing of the system has been performed by generating random combinations of sources and calculating their respective EENS and p.u.cost, after testing them through the energy management strategy that is in concern. PSO then searches for better combinations through the same process and proceeds in a direction where there exists a possibility of a global best. The optimal configuration so obtained is furnished in Table 3. The energy management strategy to meet the load demand for 24 hrs considering the wind speed, radiation, temperature data for a particular day is shown in Figure 9.

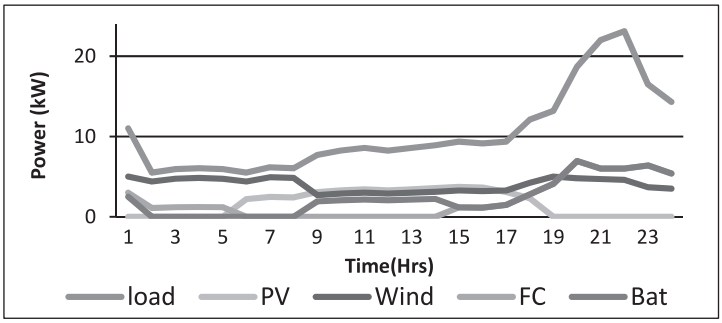

Figure 9: 24 hour demand generation curve

Table 3
Optimally Sized combination

No. of Wind Turbines	*No. of PV Modules*	*No. of Fuel cells*	*No. of Batteries*	*Electrolyzer*	*Hydrogen Storage*	*DOD*	*Pu cost*	*EENS*
1	10	1	24	1	1kg	.87	0.401	.000764

Table 4
Mean Percentage of time Occupied by Each Mode in 8760 Hours

Mode of operation	*Time (%)*
Battery mode	30.25
Fuel cell mode	6.82
Hybrid mode	43.18
Renewable recharge mode	19.75

Table 4 shows the mean percentage of time for which each mode is followed during 8760 hours. For the considered load pattern, it is observed that hybrid mode dominates .

7.2. ANN Implemented PV-MPPT

The main purpose of dynamic modeling is to observe the real time behavior of the device and also to supervise the voltage and current set points for the devices as well. The modeling processes that have been adopted in this paper have been verified by matching the calculated characteristics with that of the user manual. The choice of neurons is crucial to the accuracy of function fitting. Figure 10 displays the results of training the neural networks for three times with different number of hidden neurons with tan sigmoid function as the activation function.

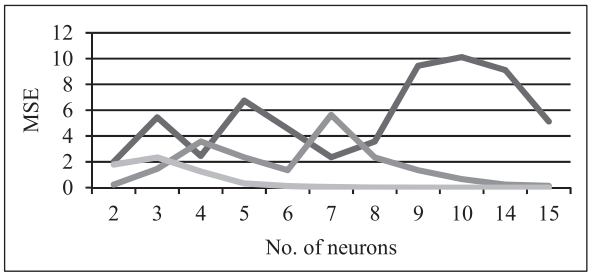

Figure 10: Choice of hidden neurons

The number of neurons are chosen on a trial and error basis and trained with different activation functions. Figure 11 is a bar graph representation of the results for training with different number of data samples and different activation functions. It is found that tan sigmoid function gives the least Mean Square Error (MSE) as compared to other activation functions.

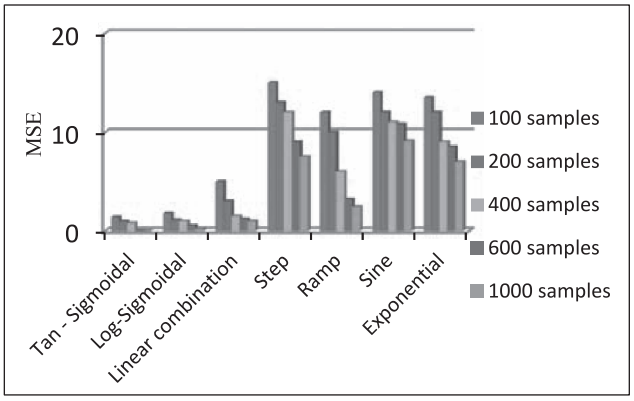

Figure 11: Choice of activation functions

TIC and TOC functions are used to determine the CPU time (elapsed time) needed to calculate the optimum voltage by the proposed MPPT algorithm and the classical P&O algorithm. As a result, the execution time of the proposed algorithm is found to be 4.98 second to calculate the optimum value of the voltage as compared to classical P&O algorithm which takes 9.7 second. This shows that the improved algorithm is faster than the classical P&O method. Figure 12 and 13 displays the reference current and Power obtained by the ANN implemented MPPT algorithm in comparison with the classical P&O method. It has been observed that the ANN method settles down smoothly at the maximum power values as compared to P&O.

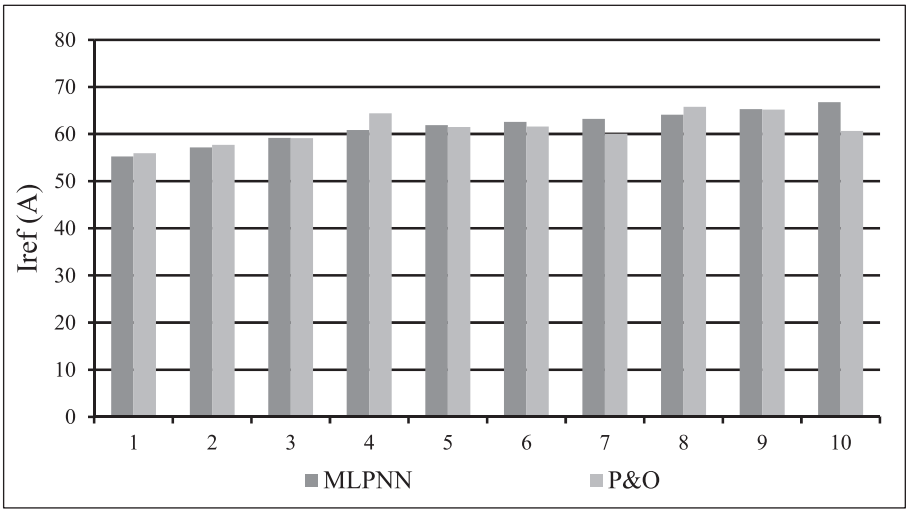

Figure 12: Comparison of I_{ref} obtained by P&O method and ANN implemented method

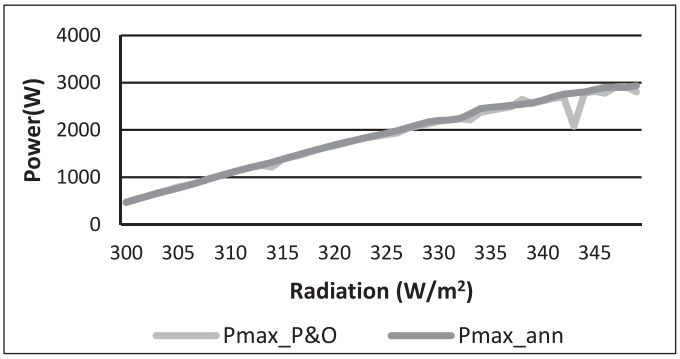

Figure 13: Comparison of power tracked by P&O method and ANN implemented method

7.3. Verification of Different Modes of Operation

Tables 5 to 9 display the technical specifications of various devices used for the simulation. The verification of the power flow control design has been done with the help of a SIMULINK model as shown in Figure 16. The block includes an embedded Matlab function that performs the energy management as given in the process of optimal sizing. Unit delays are used in order to solve the algebraic loops in SIMULINK. The SOC and volume of hydrogen constraints are checked inside the power flow control block. The following steps describe its algorithm.

Step 1: Receive PV Power at MPP and power from wind

Step 2: Check whether the load can be met by the renewable energy sources alone or not. If yes then go to step 3, else go to step 4.

Step 3: Calculate the excess power and check battery SOC conditions. If Battery SOC <= SOC_{max}, charge the batteries and thus generate a –ve Pbatref, which is then given to the battery block. Check if still remaining power exists and battery SOC = SOC_{max}. If yes, then the electrolyzer is operated to generate Hydrogen.

Step 4: Calculate the demand in excess of renewable energy and check for battery condition. If battery SOC > SOC_{min}, the battery discharges. Check if still demand is in excess of power generated or not and battery SOC <= $SOC_{min.}$ If yes then fuel cell is discharged to meet the demand.

Table 5
Technical specifications and calculated parameters for dynamic simulation of solar module

Capacity (W)	*Rs (Ω)*	T_n *K*	I_{sc} *A*	V_{oc} *V*	V_{mpp} *V*	I_{mpp} *A*	K_v *V/°C*	K_i *A/°C*
200	.7123	298	8.21	32.9	26.3	7.61	.123	.00318

Table 6
Technical specifications and calculated parameters for dynamic simulation of wind turbine

Capacity kW	$V_{cut\text{-}in}$ *m/s*	V_{rated} *m/s*	$V_{cut\text{-}out}$ *m/s*	*Efficiency*	*Cp*
5	3	10	14	.6	.6

Table 7
Technical specifications and calculated parameters for dynamic simulation of fuel cell

Capacity kW	I_{max} *A*	I_{nom} *A*	V_{nom} *V*	V_{min} *V*	E_{oc} *V*	R_{ohm} Ω	I_o *A*	*NA*
2	25	13.1	48	32	65	0.1068	0.0931	0.7977

Table 8
Technical specifications and calculated parameters for dynamic simulation of battery

Capacity Ah	E_{full} *V*	E_{exp} *V*	*A V*	*B* Ah^{-1}	*R* Ω	E_{nom} *V*	Q_{nom} *Ah*	*K V*	*Eo V*
260	13	12.7	.3	14.28	1.8	12.3	104	.6	13.29

Table 9
Technical specifications and calculated parameters for dynamic simulation of electrolyzer

Capacity kW	*Nominal Temperature °C*	*Voltage levels*	*Production rate kg/day*
2	45	48V DC ~ 220V AC	4

Figures. 15-18 display the results for the simulation of different modes. The simulation of different modes have been carried out by changing the initial values of variable parameters (initial SOC, load) at the beginning of the simulation. The battery mode is displayed in the Figure 15, where the load in excess of renewable energy is actively being met by the battery bank without the operation of a fuel cell. The SOC at the beginning of simulation has been kept at SOC_{max} due to which the fuel cell remains inactive during this period. The dynamic response of the batteries has been observed to be similar to a step response, while the battery bank voltage swings around 52V which would gradually decrease with time to reach 40V which is set as the cut-off voltage.

The Fuel cell mode becomes operational in case of long durations of very heavy load where the battery bank is completely discharged and demand in excess of renewable energy is now completely met by the fuel cell. In order to simulate this mode, the initial value of SOC has been fixed at SOC_{min}. The terminal voltage of the device varies from 54V to 36V and is taken care of by a dc-dc boost converter which steps-up the voltage to a common dc bus voltage of 230 V while the device is cut-off at 35V.

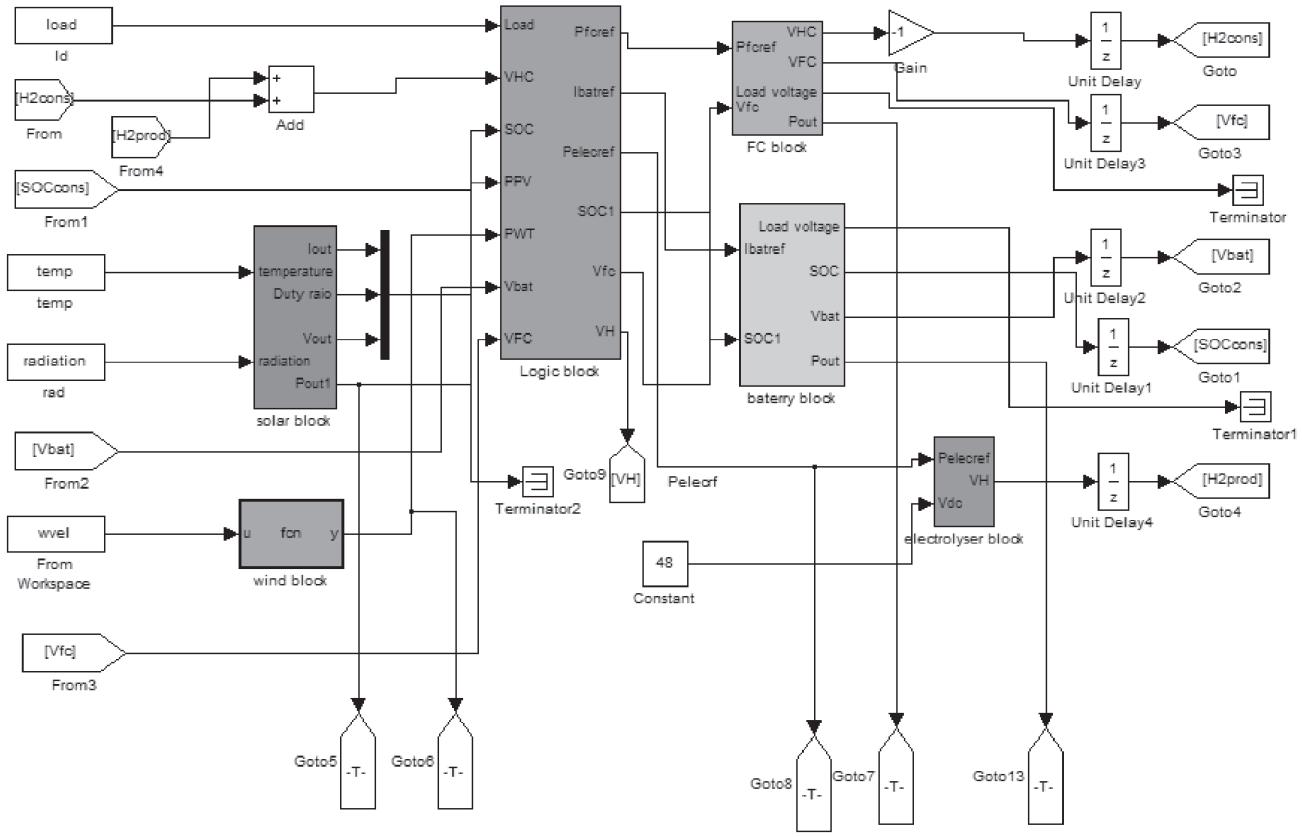

Figure 14: Simulink Model for the system design

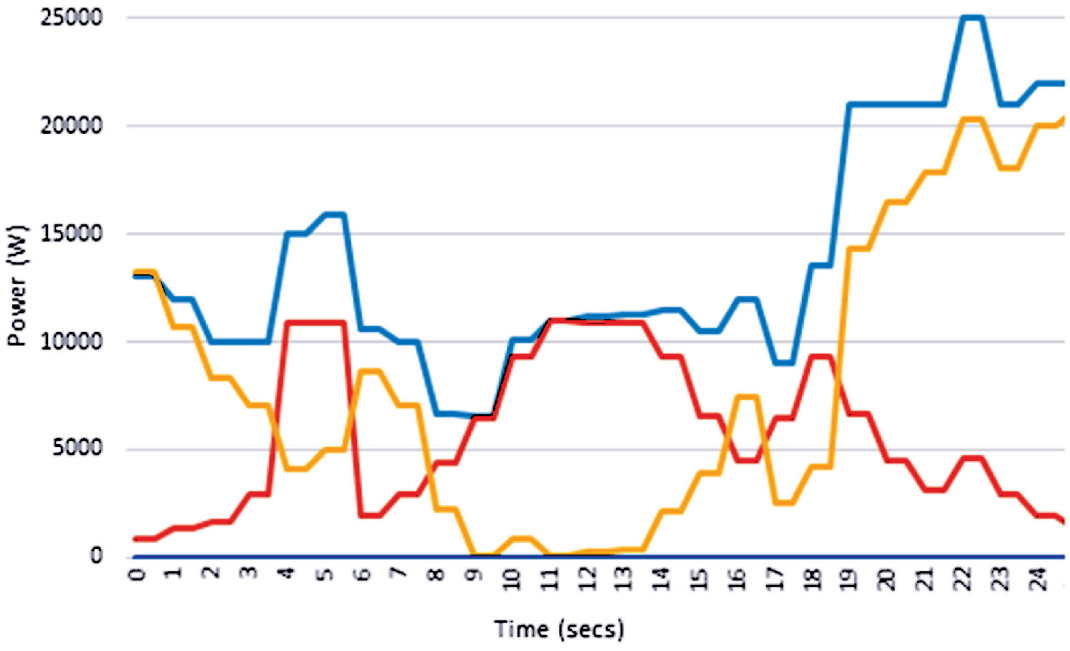

Figure 15: Battery mode

The hybrid mode plays the most crucial role in the entire energy management strategy by improvising the load sharing where in the load is halved between the battery and the fuel cell. In order to simulate this mode,

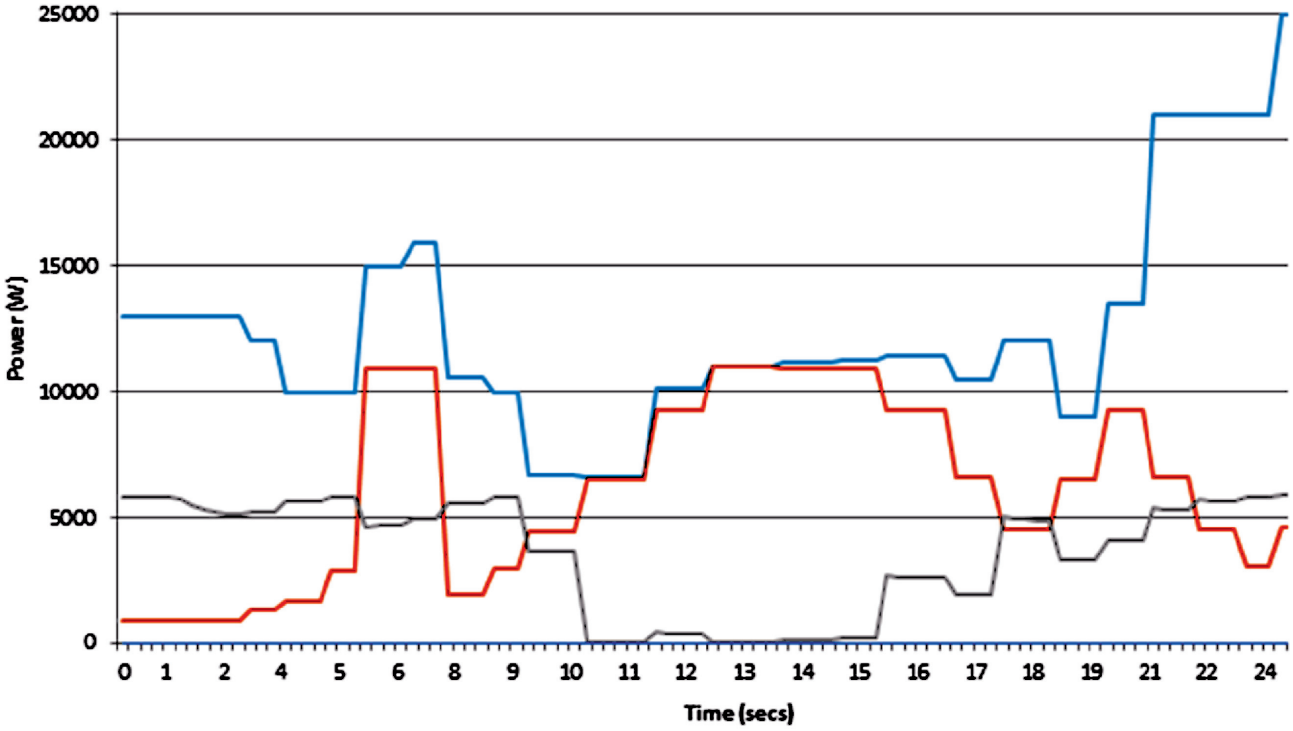

Figure 16: Fuel cell mode

SOC has been kept just above SOC_{min} so that even with maximum discharge the battery will not be able to meet the load. From 13 to 18 seconds the load is moderate and is halved between the battery and fuel cell but as the load spikes, the equal division of load is no more maintained but the hybrid mode is retained such that the fuel cell operates at its maximum capacity, while the rate of change of battery SOC is greatly reduced. Renewable recharge mode is followed when renewable energy is in excess of load or during very lightly loaded periods which occur during the morning period of the day.

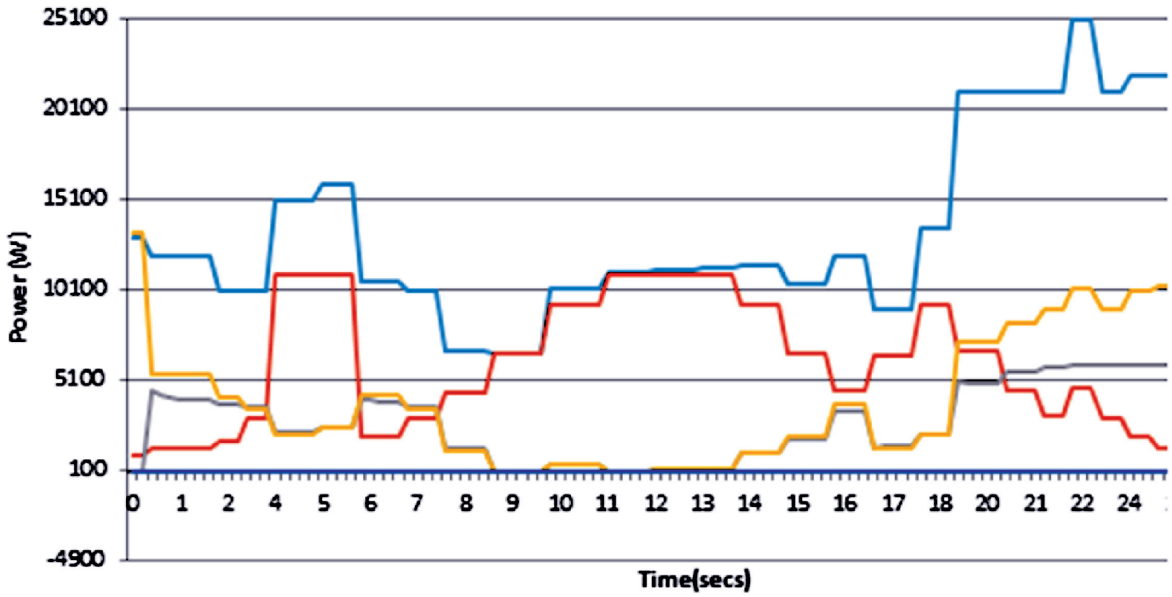

Figure 17: Hybrid mode

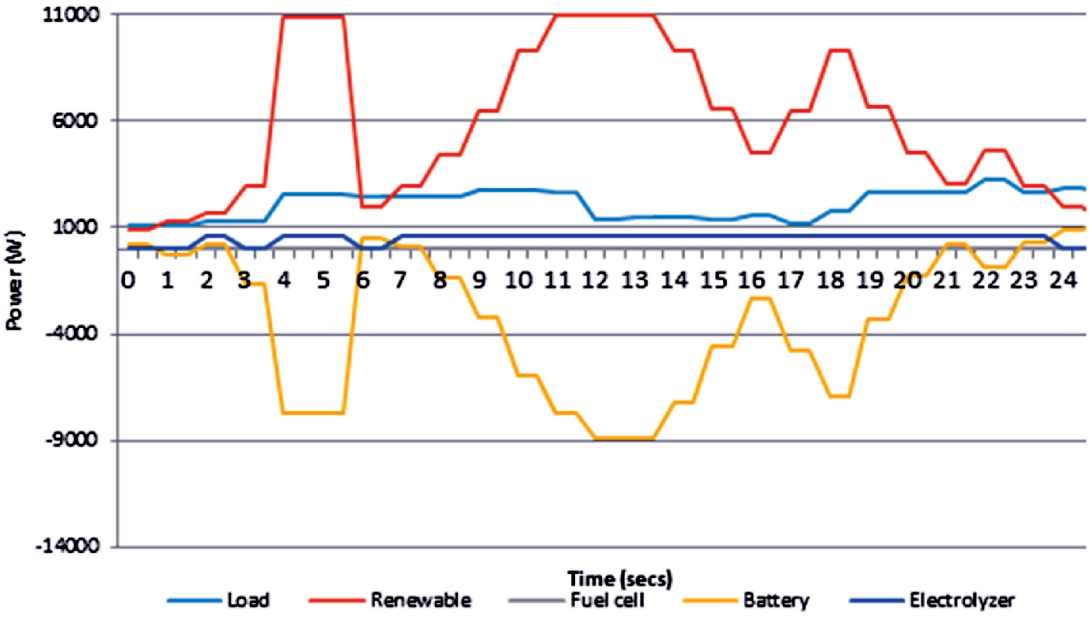

Figure 18: Renewable recharge mode

8. CONCLUSION

This paper deals with optimal sizing of a wind/PV/fuel cell/battery system using PSO, where, the number of wind turbines, number of PV modules, number of batteries, number of fuel cells, volume of hydrogen to be stored and DOD of the battery bank have been optimized, by developing a single objective function consisting of two objectives: EENS (for reliability) and per unit cost. The optimal configuration has then been simulated, using dynamic modeling, to verify the different modes of operations. The real time simulation and the optimal sizing of the combination has been performed for a standard domestic load. Importance is given to the new energy management strategy which implements a feed-forward ANN trained with Levenberg – Marquardt algorithm for MPPT of PV modules .It calculates the reference power for batteries and fuel cells based on the terminal voltage and discharge current satisfying the SOC and volume of hydrogen constraints. The terminal voltage of both the power storage equipments has been monitored and found to be within the acceptable limit. A comparison has been made between the classical P&O MPPT and the ANN implemented MPPT where the mean efficiency of the ANN implemented method has been found to be better than that of P&O implemented method.

REFERENCES

[1] A. Yiannis Katsigiannis, S. Pavlos Georgilakis, S. Emmanuel Karapidakis. Hybrid Simulated Annealing-Tabu Search Method For Optimal Sizing Of Autonomous Power Systems With Renewable. *IEEE transactions on sustainable energy*, Vol. 3, pp. 3, 2012.

[2] Daming Xu, Longyun Kang, Liuchen Chang BinggangCo. Optimal sizing of standalone hybrid wind/PV power systems using genetic algorithms. *Electrical and Computer Engineering. IEEE Canadian Conference*, Saskatoon, 2005.

[3] Eftichios Koutroulis, Dionissia Kolokotsa, Antonis Potirakis, Kostas Kalaitzakis. Methodology for optimal sizing of stand-alone photovoltaic/ wind generator systems using genetic algorithms. *Elsevier Solar Energy Journal*, Vol. 80, No. 9, pp. 1072-1088, 2006.

[4] G.J. Dalton, D.A. Lockington, T.E. Baldock. Case study feasibility of renewable energy supply options for small to medium size tourist accommodations. *Renewable Energy*, Vol. 34, No. 4, pp. 1134-1144, 2009.

[5] R.O. Belfkira Hajji, C. Nichita, G. Barakat. Optimal sizing of a stand-alone hybrid wind/PV system with battery storage. *Proceedings of Power Electronics and Applications .IEEE European Conference*, Aalburg, September 2-5, 2007.

[6] Jidong Wan, Fan Yang .Optimal capacity allocation of standalone wind/PV/battery hybrid power system based on an improved particle swarm algorithm. *IET Renewable Power Generation*, Vol. 3, No. 5, pp. 443-448, 2013.

[7] Eiben, A.E., P.E. Raue. Genetic algorithms with multi-parent recombination used for optimal sizing of a standalone wind/PV system. *Proceedings of the International Conference on Evolutionary Computation*. *The Third Conference on Parallel Problem Solving from Nature*, pp. 78-87,1994.

[8] Toshiro Hiros, H .Matsuo. Standalone Hybrid Wind-Solar Power Generation System Applying Dump Power Control Without Dump Load. *IEEE transactions on industrial electronics*, Vol. 59, No. 2, pp. 988-997, 2012.

[9] Chun-Hua Li, Xin-Jian Zhu, Guang-Yi Cao, Sheng Sui, Ming-Ruo Hu. Dynamic modeling and sizing optimization of stand -alone photovoltaic power systems using hybrid energy storage technology. *Renewable Energy, Elsevier*, Vol. 34, 2009.

[10] Benhachani.Z, B. Azomi, R. Abdessemed, M. Chabane. Optimal sizing of a Solar-Wind Hybrid Farm Supplying a Farm in a Semi – Arid Region in Algeria. *Proceedings of Universities of Power Engineering Conference*, 2012.

[11] H. Yang, W. Zhou, C. Lou. Optimal design and techno-economic analysis of a hybrid solar–wind power generation system. *Applied Energy*, Vol. 86, No. 2, pp. 163-169, 2009.

[12] P. Ylmaz, Hakan Hocaoglu, M. Konukman, A.E.S.A prefeasibility case study on integrated resource planning including renewables. *Energy Policy*, Vol. 36, No. 3, pp. 122301232, 2008.

[13] S. Diaf, G. Notton, M. Belhamel, M. Haddadi, A. Louche. Design and techno-economical optimization for hybrid PV/wind system under various meteorological conditions. *Applied Energy*, Vol. 85, No. 10, pp. 968-987, 2008.

[14] K.J. Runtz, M.D. Lyster. Fuel Cell Equivalent Circuit Models For Passive Mode Testing and Dynamic Response. *IEEE conference on Electrical and computer Engineering*, Saskatoon, May 1-4, 2005.

[15] Marcello Gradella Villalva, J.R. Gazoli, E.R. Filho. Comprehensive approach to modeling and Simulation of Photovoltaic Arrays. *IEEE transaction on power electronics*, Vol. 24, No. 5, pp. 1198-1208, 2009.

[16] Olivier Trembley, Louis A. Dessaint, Abdel Illah Dekkiche. A Genereic Battery Model for Dynamic Simulation of Hybrid Electric Vehicles. *IEEE Vehicle Power and Propulsion Conf*., Arlington, September 2007.

[17] Yu Qiuli, K. Anurag Srivastava, Song-Yul Choe, Wenzhong Gao. Improved modeling and control of a PEM fuel cell power system for vehicles. *Proceedings of the IEEE, Southeast Conf,* pp. 331 - 336, March 31- April 2, 2006.

[18] K. Levenberg, A method for the solution of certain problems in least squares, *Quarterly of Applied Mathematics,* Vol. 5, pp. 164-168, 1944

[19] J. Zorilla Casanova, M. Piliougine, J. Carretero, P. Bernala, P. Carpena, L. Mora Lopez, M. Sidrach-de-cardano. Analysis of Dust losses in Photovoltaic modules. *World Renewable energy congress*, Linkoping, Sweden, May 8-13, 2011.

[20] Hussein A Kazem, Tamer Khatib, K.Sopian,Frank Buttinger, Wilfried Elmenreich, Ahmed Said Albusaidi. Effect of dust deposition on the performance of multi-crystalline Photovoltaic modules based on experimental Measurements. *IJRER*,. Vol. 3, No. 4, 2013.

[21] Christina Honsberg, Stuart Bowden.,*www. Pveducation .org.*

[22] Souleman Njoya M, Olivier Tremblay, Louis A. Dessaint. A Generic Fuel Cell Model For Simulation of Fuel Cell Power Systems. *IEEE Power and Energy Society General meeting*, Quebec, Canada, July 2009.

[23] J. Kennedy, R. Eberhat. Particle Swarm optimisation. *Proceedings of IEEE International conference on Neural Networks*, November 27, 1995.

[24] David Sanz Morales. Maximum power point tracking algorithms for photovoltaic applications. Alto University. Thesis for Masters.

[25] Soumyadeep Nag, Namitha Philip.Application of ANN to Automatic Load frequency control. *Springer Journal LNCS*, Vol. 2928, 2013.

[26] Lin Xu, Xinbo Ruan, Chengxiong Mao, Buhan Zhang, Yi Luo. An improved optimal sizing method for wind-solar-battery hybrid power system. In *Proceedings of IEEE transactions on sustainable energy*, Vol. 4, No. 3, pp. 774-785, 2013.

[27] Bingjun Xiao, Yiyu Shi, Lei He. A universal state of charge algorithm for batteries. In *Proceeding of DAC'10 conference*, California, June 13-18, 2010.

[28] Hisham El Khashab,Mohammed Al Ghamedi .Comparison between hybrid renewable energy systems in saudi Arabia. *Journal of Electrical systems and Information Technology*. Vol. 2, No. 1, pp. 111-119, May 2015.

[29] Y.V. Pavan kumar, Ravikumar Bhimasingu. Renewable energy based microgrid system sizing and energy management for green building.*Journal of modern Power systems and clean energy.* Vol. 3, No. 1, pp. 113, March 2015.

[30] Z. Abdin, C.J. Webb, E. Mac A. Gray. Solar hydrogen hybrid energy systems for off-grid electricity supply: A critical review. *Renewable and sustainable energy reviews.* Vol. 52, pp. 1791-1808, 2015.

[31] Wu.Z. Tazvinga, X. Xia. Demand side management of photovoltaic -battery hybrid system. *Applied Energy*, Vol. 149, pp. 294-304, 2015.

[32] T. Kamal, S.Z. Hassan, L. Khan, S. Mumtaz. Energy management and control of grid connected Wind/Fuel Cell/battery hybrid renewable energy system. In P*roceedings of IEEE conference on Intelligent systems Engineering,* 2016.

[33] M. Espinosa Trujillo, M. Flota Banuelos, D. Pacheco Catalan, M. Smit, Y. Verde Gomez. A novel stand alone mobile photovolatic/wind turbine/ultracapacitor/battery band hybrid power system. Journal of renewable and sustainable energy. Vol. 7, No. 2, 2015.